

Title: Development of probability of detection data for structural health monitoring damage detection techniques based on acoustic emission

Authors: ¹Daniel Gagar
¹Phil Irving
¹Ian Jennions
²Peter Foote
²Ian Read
³Jim McFeat

ABSTRACT

Structural Health Monitoring (SHM) techniques have been developed as a cost effective alternative to currently adopted Non-Destructive Testing (NDT) methods which have well understood levels of performance. Quantitative performance assessment, as used in NDT, needs to be applied to SHM techniques to establish their performance levels as a basis for technique comparison and also as a requirement for practical aerospace application according to set regulations. One such measurand is Probability of Detection (POD). This paper reports experiments conducted to investigate the location accuracy of the Acoustic Emission (AE) system in monitoring events from Hsu-Nielson and fatigue crack AE sources as a route to establish the POD of AE in SHM. It was found that fatigue crack tips could be located at 90% POD within 10 mm accuracy.

INTRODUCTION

Application of traditional NDT inspection techniques to ensure the continued airworthiness of safety critical structures such as aircraft relies on quantitative data describing their sensitivity to damage and the Probability of Detection (POD) of specified damage levels. Civil aircraft use a damage tolerant approach to structures. Here the service life before the first inspection and the length of subsequent inspection intervals are determined by the size that a defect would have reached during that period. Inspections should detect such a defect with 90% POD and 95% confidence. Quantitative data on the relation between POD and damage size and the associated confidence level has been established for all commonly used NDT techniques such as eddy current, ultrasonics and even visual inspection [1].

Application of automated Structural Health Monitoring (SHM) techniques to replace or augment manual NDT will require the development of equivalent quantitative POD data. It becomes even more vital if health monitoring data is to be used as part of a prognostic life assessment and enhanced maintenance methodology. An essential input to calculations of future service life will be a measurement of damage state, expressed in terms of probability of detection of the current damage level. Published data on reliability of damage detection for

¹ Cranfield University IVHM Centre, Cranfield, Bedfordshire, UK. MK43 0AL

² BAE Systems, ATC-Sowerby, FTC 267, PO Box 5, Filton, Bristol, UK

³ BAE Systems, Warton Aerodrome, Lancashire, UK. W427D

SHM monitoring techniques generally has little quantitative information of their performance expressed in POD and confidence terms.

As part of a wide programme of research to quantify and validate damage detection techniques for health monitoring application, damage sensing techniques related to the Acoustic Emission (AE) approach have been investigated to quantify their POD performance levels.

Acoustic emission is used both to sense the presence of damage via acoustic waves- and also to locate the damage. Thus there are two POD/ confidence curves for a given AE setup, one related to the size or severity of the damage, the other related to the damage location error. The work described in this paper refers to the location POD.

EXPERIMENTS

Experiments were conducted to investigate the location accuracy of the AE system using two types of AE source: a Hsu-Nielson source and a fatigue crack source. A Physical Acoustics 4-channel acoustic emission system (PCI2) equipped with WDI broad band piezoelectric sensors was used to record the AE data which was conditioned, filtered and amplified with a 40 dB_{AE} gain (0 dB_{AE} Ref. 1 μ V/sensor); sensor coupling to the sample was achieved using Dow Corning RTV 3140 silicone rubber. The accompanying AEWin software package was used to control the acquisition setup and perform other signal processing functions.

(1) Hsu-Nielson AE Source

A Hsu-Nielson (HN) source was used to generate AE events in a plain aluminium sample with the following setup configurations: (i) three AE sensors spaced 390 mm apart in a triangular formation on a 450x550 mm 2014A aluminium sample; (ii) four AE sensors spaced 390 mm apart, in a square formation on a 450x550 mm 2014A aluminium sample; (iii) three AE sensors spaced 780 mm apart in a triangular formation on a 1x2 m 2014A aluminium sheet. The test trials were performed by making arrays of pencil lead breaks at predetermined locations across the area of the samples, estimating location using the time of arrival algorithm, with detection threshold set at 49 dB_{AE}.

The time-of-arrival (TOA) algorithm is used for determining the location of AE events in 2D. This functionality is built in the Physical Acoustics system; it is based on the relationship between the propagating wave velocity, distance and times of arrival of the signals at known sensor locations. The performance of the system in locating AE event is heavily dependent on the accuracy of timing measurement which is calibrated to 1 μ s or approximately 5 mm.

(2) Fatigue Crack AE Source

The AE system was used to detect and locate acoustic emissions from a growing fatigue crack. The test specimen was 2 mm thick 2014 aluminium alloy 530 mm long and 250 mm wide. A 10 mm notch was placed on the sample edge at the mid-point between sample ends. The sample was subjected to constant amplitude sinusoidal loading at an R ratio (R= minimum stress/maximum stress) of 0.1 with maximum stress of 52 MPa. All tests were performed in a servo

hydraulic fatigue machine at a frequency of 2 Hz. Loads were measured to an accuracy of 0.1 % of maximum load.

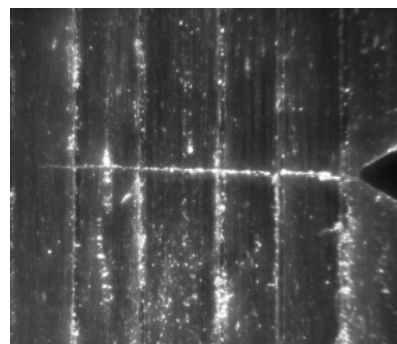
The fatigue crack initiated at the notch root and propagated perpendicularly to the applied load across the sample width. Prior to testing one side of the sample was polished and marked with scribes at 1 mm intervals to facilitate monitoring of the crack length. A digital video system was used to capture images of the crack, with an appended timestamp, as it progressed across the sample. Image frames were recorded at intervals of 150 cycles and were used in post test analysis to determine crack length from initial crack initiation to final failure. Crack length could be measured to an accuracy of ± 0.3 of a mm.

Two setup configurations were used in this experiment: (i) two AE sensors positioned at locations (125,135) mm and (125, 335) mm on the sample for linear location of AE events (ii) four AE sensors positioned at locations (185, 225) mm, (185, 340) mm, (64, 342) mm and (66, 225) mm for 2D location of AE events. Exclusive detection of AE from the fatigue crack in the linear location setup was ensured by implementing a timing filter, based on time difference of arrival of AE between sensors, which restricted AE acquisition and location to a defined region of the sensor array. The general setup is illustrated in Figure 1.

Experiments were performed by beginning recording AE data as the loading on the test sample commenced using a detection threshold of 49 dB_{AE}. The influence of a fixed detection threshold on location accuracy was investigated by re-processing the acquired data at various levels of detection threshold. A total of three fatigue samples were tested using the same mechanical loading and data acquisition settings; two in the linear AE location setup and one in the 2D AE location setup.



(a)



(b)

Figure 1: (a) General setup of fatigue crack AE event monitoring experiment (b) crack initiation from sample notch with inscribed markings at 1 mm intervals

Once the tests were complete, the predicted locations of the Hsu-Nielson or fatigue crack AE events were computed using the TOA algorithm previously described. This was compared with the actual location of the crack tip or Hsu-Nielson source and an error vector calculated. Errors were ranked and the cumulative probability of detection determined by the expression below and plotted against errors.

$$P(x_i) = \frac{\text{number of observations} \leq x_i}{n + 1}, \quad x_1 \leq x_2 \leq \dots \leq x_n \quad (1)$$

In the case of the 2D fatigue crack AE setup, the computed AE event locations were analyzed using Kernel Density Estimation (KDE) [2] to monitor the trend of AE activity during the test.

RESULTS

(a) Hsu-Nielson AE Source

The results of these experiments are summarized in Table I and illustrated in Figures 2 and 3. Figure 2 shows a plan view of the aluminium sample used for Hsu-Nielson AE event location test with the actual and estimated AE event locations shown. It is clear that the minimum errors are in the middle of the sheet and the largest errors towards the edge.

Figure 3 shows the cumulative frequency of error margin plotted against error for the Hsu-Nielson AE events location tests. This shows that best location accuracy is obtained using four sensors. On the 450 X 550 mm sample 90% of the errors were less than 6 mm. Reducing the number of sensors to three increased this figure to 11 mm, and using three sensors on a larger 1 X 2 m sheet increased the error further to 16 mm. Also, it is observed from Table I that the test setup with the highest average amplitude and the least variance gave the best AE event location performance.

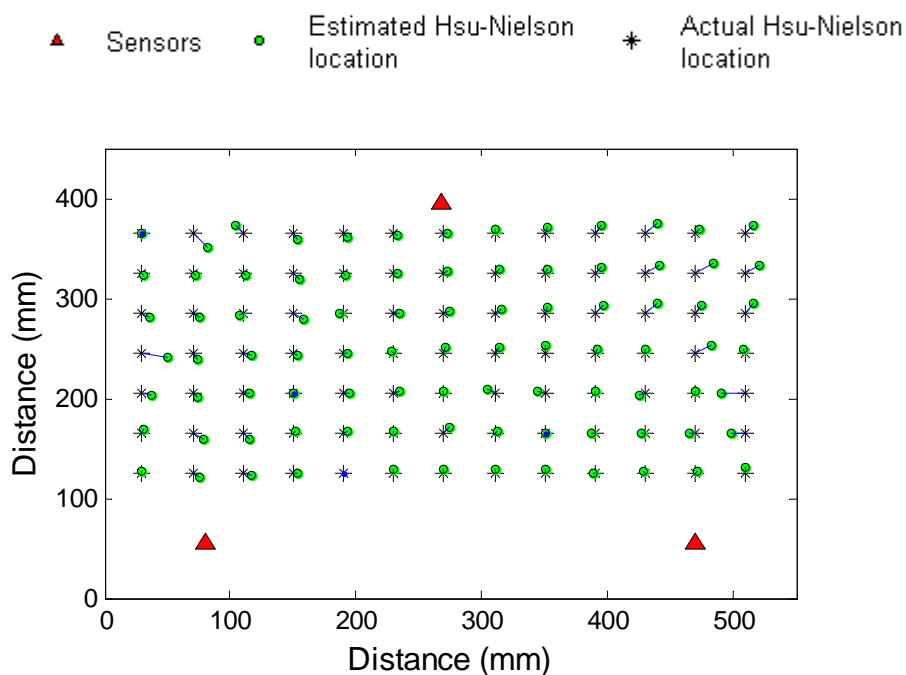


Figure 2: Hsu-Nielson source location using the AE system

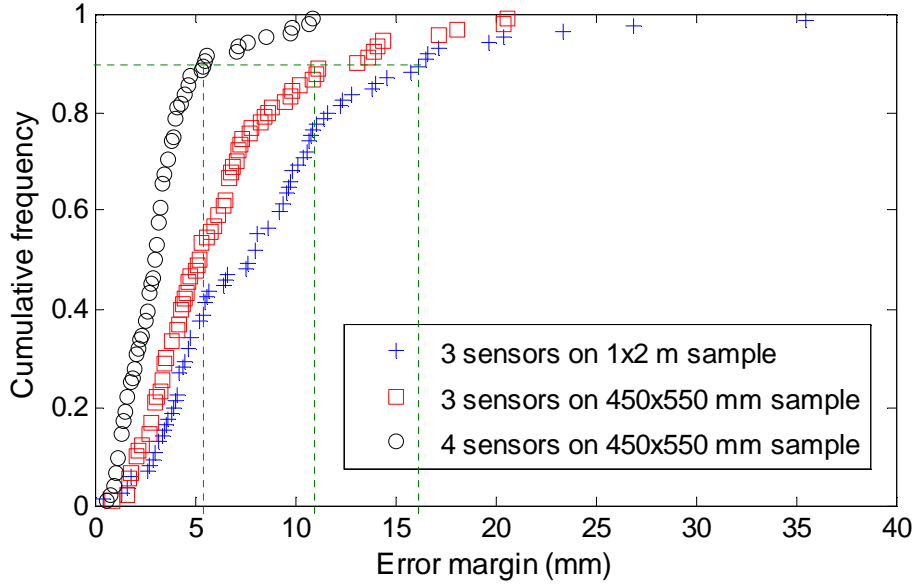


Figure 3: Cumulative frequency of error margins with various experimental configurations using Hsu-Nielson AE source

Table I: Results summarizing location performance of the AE system in monitoring Hsu-Nielson events

Setup configuration	Maximum error (mm)	Minimum error (mm)	Error margin at 90% cumulative frequency (mm)	Amplitude	
				Mean (dB _{AE})	Coefficient of variance
3 sensors on 450x550 mm	20.6	1.6	11.2	89.6	0.06
4 sensors on 450x550 mm	10.6	0.6	5.4	91	0.04
3 sensors on 1x2 m	35.5	0.4	16.3	82.8	0.07

(b) Fatigue Test Results

The fatigue crack initiated easily from the notch and propagated across the sample, without deviation. It was found that there was considerable scatter in the predicted data points of AE events monitored during the tests as illustrated in Figure 4. This shows the KDE plots of cumulative AE activity during the fatigue test using the 2D AE event location setup; 4(a) is a 3D contour and 4(b) plot is a plan view of the sample. The crack was initiated at the middle of the right-hand edge of the plate and propagated across it until failure. This trend of the crack growth path can be observed from these plots.

The results of AE monitoring from fatigue crack experiment using the linear AE event location setup is summarized in Table II and illustrated in Figures 5 and 6.

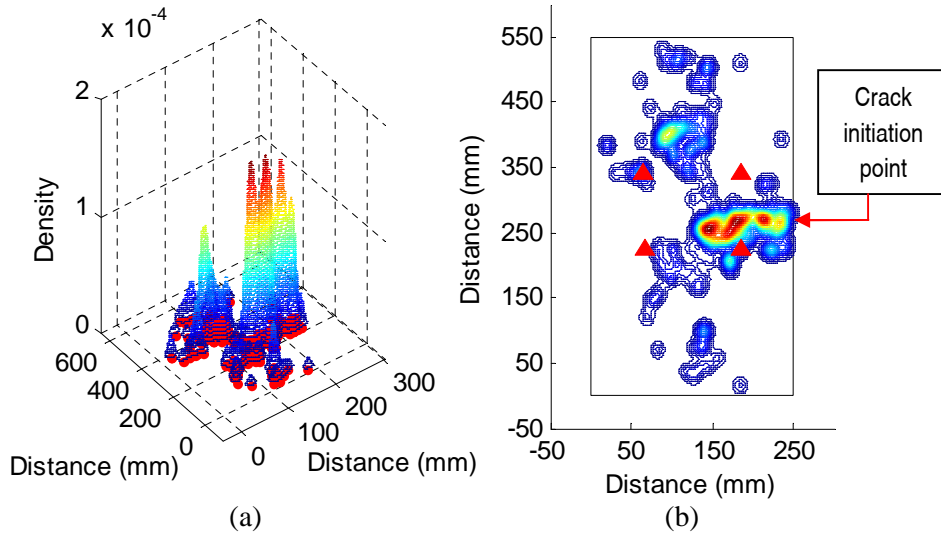


Figure 4: KDE plots of cumulative AE activity during fatigue test using 2D AE location setup

Figure 5 and 6 show the cumulative frequency of error margin plotted against error for the fatigue tests using the linear AE event location setup. It is observed that increasing the detection threshold resulted in better location performance. Figure 7 and Table II summarizes the results from the tests and it shows that that the settings that gave the highest average amplitude and the least variance gave the best AE event location performance. Table II also shows crack lengths at first AE detection which are approximately between 1 - 3 mm, suggesting a good sensitivity to early detection of fatigue cracks.

Table II: Results summarizing location and detection performance of the AE system in monitoring fatigue crack generated AE events using the linear location setup

(a) Test 1

Detection threshold	Error margin at 90% cumulative frequency (mm)	Earliest crack detection (mm)	Amplitude	
			Mean (dB _{AE})	Coefficient of Variance
49	32	< 1	69	0.18
55	28	2	73	0.13
60	19	2.5	76	0.09
65	10	2.5	78	0.07

(b) Test 2

Detection threshold	Error margin at 90% cumulative frequency (mm)	Earliest crack detection (mm)	Amplitude	
			Mean (dB _{AE})	Coefficient of Variance
49	19	2.5	57.5	0.06
55	7	2.6	59	0.04
60	7	2.8	61.3	0.03
62	9	3.5	63.1	0.02

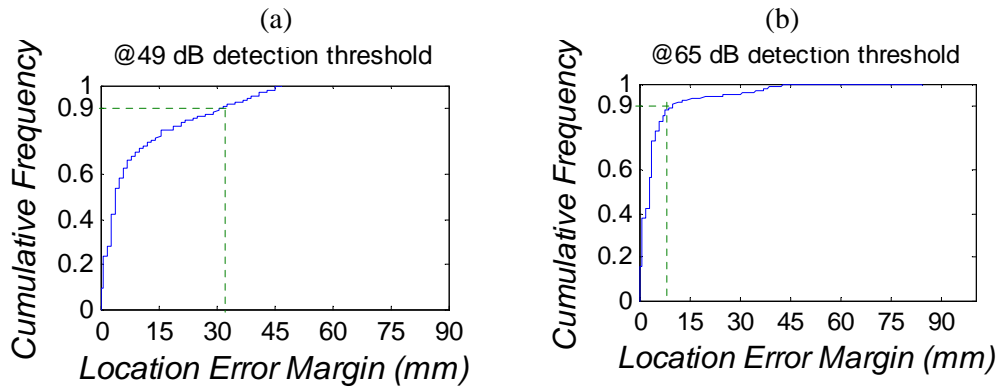


Figure 5: Cumulative frequency of location error margins and AE data trend at various detection thresholds from Test 1, using the linear location setup (a) 49 dB_{AE} (b) 65 dB_{AE}

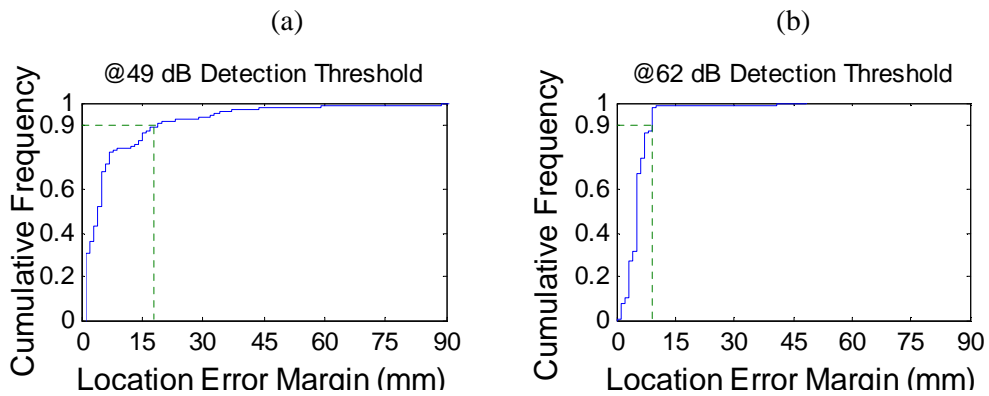


Figure 6: Cumulative frequency of location error margins and AE data trend at various detection thresholds from Test 2, using the linear location setup (a) 49 dB_{AE} (b) 62 dB_{AE}

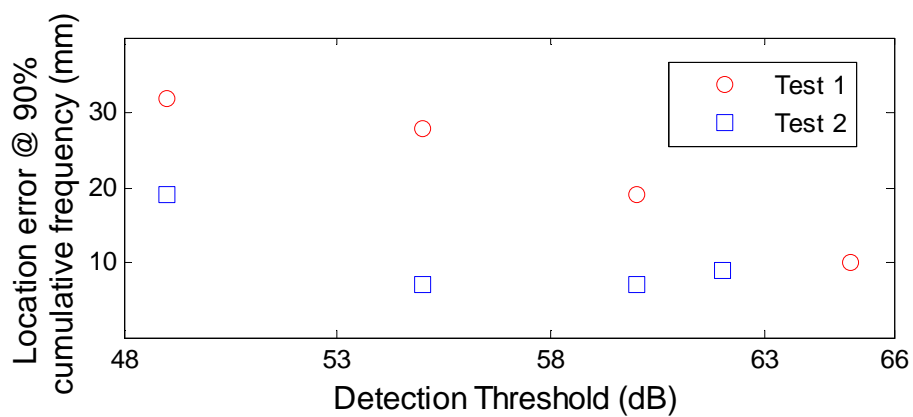


Figure 7: Cumulative frequency of location error margins and AE data trend at various detection thresholds from Test 1 and Test 2, using the linear AE location setup

DISCUSSION

The location accuracy of the AE system in localizing AE events is a function of the source of AE signals monitored, the material properties of the propagating medium, the data acquisition hardware and as well as the computation algorithms. Combinations of these factors in various scenarios contribute to different levels of the AE system location accuracy performance.

In the Hsu-Nielson event location experiments, the location accuracy is most markedly influenced by the number of sensors and the distance between them; this is because an additional sensor to an array of sensors introduces an additional variable for the same mathematical problem, creating an over-determined solution.

It is observed in Table II that the AE system is capable of detecting fatigue cracks of less than 1 mm, which is comparable to the performance of its pre-existing NDT counterparts like Dye Penetrant and Wire Crack Gauge capable of 0.25 mm and 0.1 mm respectively [1]. However, as with other NDE techniques, this performance requires a probabilistic representation to conform to the guidelines set by aviation regulators. This would require repeat tests in similar monitoring conditions and operating procedures to establish confidence intervals.

The trend of the cumulative AE activity illustrated in Figure 7 also shows AE activity registered in regions not correlated with the crack path. The factors which influence this occurrence are currently under investigation.

Future work in this research theme includes further study on POD models for AE as well as validation and verification trials on test structures with representative geometry and features of practical engineering applications.

CONCLUSIONS

- (1) AE source location experiments in aluminium sheet using TOA algorithms can locate fatigue cracks with 90% of the measured errors less than 32 mm with a detection threshold of 49 dB_{AE}.
- (2) Increasing the threshold level to 65 dB_{AE} decreases the maximum error for 90% of the determinations to 10 mm.

ACKNOWLEDGEMENTS

This study is sponsored by the Cranfield University IVHM Centre.

REFERENCES

- [1] Wheatley, G., Kollgaard, J., Register, J. and Zaidi, M. (2003), "Comparative vacuum monitoring as an alternate means of compliance", *Proceedings of the 4th International Workshop on Structural Health Monitoring, Stanford University, Stanford, CA, September 15-17, 2003*
- [2] Simonoff, J. S. (1996), *Smoothing methods in statistics*, Springer, New York.

2013-12-12

Development of probability of detection data for structural health monitoring damage detection techniques based on acoustic emission

Gagar, Daniel

Stanford University

Gagar, D. et al. (2013) Development of Probability of Detection Data for Structural Health Monitoring Damage Detection Techniques Based on Acoustic Emission, Proceedings of the 8th International Workshop on Structural Health Monitoring, Stanford, United States of America, 13-15 September 2011, pp. 1391-1398

<https://dspace.lib.cranfield.ac.uk/handle/1826/9993>

Downloaded from Cranfield Library Services E-Repository